J. Physiol. (1986), **378**, *pp.* 313–334
With 9 text-figures
Printed in Great Britain

CALCIUM AND LONG-TERM TRANSMISSION DAMAGE FOLLOWING ANOXIA IN DENTATE GYRUS AND CA1 REGIONS OF THE RAT HIPPOCAMPAL SLICE

BY IRA S. KASS* AND PETER LIPTON†

*From the †Department of Physiology, University of Wisconsin, Madison, WI 53706, U.S.A. and the *Department of Anesthesiology, State University of New York, Health Science Center, Brooklyn, NY 11203, U.S.A.*

(*Received 1 August 1985*)

SUMMARY

1. The mechanism of long-term anoxic damage in brain tissue is investigated using the rat hippocampal slice as a model system. The effects of short durations of anoxia on subsequent transmission through two neural pathways are studied. 10 min of anoxia irreversibly abolishes transmission between the perforant path and the dentate granule cells while only 7 min of anoxia irreversibly abolishes transmission between the Schaeffer collaterals and the CA1 pyramidal cells. We examine the involvement of Ca^{2+} in this irreversible transmission damage and, also, the differential sensitivities of the dentate gyrus and CA1 regions.

2. Substitution of a buffer containing 0 Ca^{2+} and 10 mM-Mg^{2+} during the anoxic period substantially improves the recovery of synaptic transmission in both regions of the slice. Dentate gyrus transmission recovers completely after 20 min of anoxia and CA1 transmission survives 10 min of anoxia. These results suggest that Ca^{2+} influx during anoxia may be an important cause of the long-term damage.

3. The uptake of $^{45}Ca^{2+}$ into the intracellular space of the slice is increased during anoxia. This effect is approximately twice as large in CA1 as in the dentate gyrus. Thus, in the dentate gyrus the calculated exchangeable pool of Ca^{2+} is increased 30% by anoxia and in the CA1 it is increased by 70%.

4. Two incubating conditions which decrease the amount of $^{45}Ca^{2+}$ uptake during anoxia protect transmission against long-term damage. (a) Pre-incubation of the slices with 25 mM-creatine elevates tissue phosphocreatine and attenuates the fall in adenosine 5′-triphosphate (ATP) during anoxia. This is associated with partial protection against transmission damage and an approximate 50% attenuation of the anoxic uptake of $^{45}Ca^{2+}$. (b) Inclusion of 2 mM-cobalt in the buffer reduces the normoxic uptake of $^{45}Ca^{2+}$ so that the uptake during anoxia is no greater than normoxic uptake in the absence of cobalt. This is associated with a complete protection against long-term transmission damage following 10 min of anoxia in the dentate gyrus.

5. A kinetic analysis of the $^{45}Ca^{2+}$ uptake shows that the anoxic uptake results primarily from inhibition of the unidirectional efflux of Ca^{2+} from the cells; there is no calculable increase in the undirectional influx. This suggests that anoxia increases

Ca^{2+} uptake by inhibiting one or more Ca^{2+}-extrusion processes and not by opening depolarization-sensitive Ca^{2+} channels. This inference is supported by the action of the 2 mM-cobalt. While this ion almost completely blocks veratrine-induced $^{45}Ca^{2+}$ uptake it has no effect on the anoxic increase in $^{45}Ca^{2+}$ uptake in the dentate gyrus and only a 15% inhibitory effect on the anoxic increase in $^{45}Ca^{2+}$ uptake into CA1.

6. 3×10^{-6} M-ouabain decreases cell K^+ and elevates cell Na^+ more than does 10 min of anoxia yet it has no effect on $^{45}Ca^{2+}$ uptake. This (a) supports the inference that depolarization during anoxia is not the factor leading to increased Ca^{2+} uptake and (b) suggests that the Na^+–Ca^{2+} exchange mechanism is not the extrusion process which is inhibited during anoxia.

7. The data are consistent with, and support, the following explanation for long-term transmission damage following anoxia: a fall in neuronal ATP leads to inhibition of the Ca^{2+}-ATPase-driven extrusion pump and a subsequent rise in intracellular Ca^{2+}. This increase in cell Ca^{2+} (possibly in conjunction with other factors) leads to the events which cause long-term damage to the transmission process. The enhanced vulnerability of transmission in CA1 to anoxia results from a larger net uptake of Ca^{2+} in CA1 than in the dentate gyrus during anoxia. This, in turn, results largely from a more profound inhibition of the Ca^{2+}-ATPase but, also, from a small increase in Ca^{2+} influx through depolarization-sensitive channels.

8. Neither the mechanism by which Ca^{2+} is acting, nor the reason that $^{45}Ca^{2+}$ uptake during anoxia is larger in CA1 than in the dentate gyrus, are known. With regard to the former, measurements of the fall in ATP during anoxia, and the effects of omitting Ca^{2+} on that fall, suggest that Ca^{2+} does not exert its toxic effect by enhancing the fall in ATP. With regard to the latter, the percentage fall in ATP during anoxia is no larger in CA1 than it is in the dentate gyrus.

9. In an appendix we present a kinetic analysis of $^{45}Ca^{2+}$ uptake into a cell containing a very small cytosolic Ca^{2+} pool and a large, kinetically homogenous, organelle-localized pool of exchangeable Ca^{2+}.

INTRODUCTION

Between 10 and 15 min of exposure to anoxia causes irreversible morphological (Pulsinelli, Brierly & Plum, 1982; von Lubitz & Diemer, 1983) and functional (Keykhah, Welsh, Miller, Harp & Defoe, 1978; Smith, Kagstrom, Rosen & Siesjo, 1983) damage to brain tissue. While large decreases in cerebral pH will apparently cause such damage (Myers, 1981; Rehncrona, Rosen & Siesjo, 1981) the damage normally occurs in the absence of such large increases in acidity (Siesjo, 1981). Among other possible triggers for this irreversible damage is an increase in cytosolic Ca^{2+}. This has been suggested by several groups of workers (Siesjo, 1981; Hass, 1981; Meldrum, 1981) and there is a large decrease in extracellular Ca^{2+} during ischaemia *in situ* (Harris, Symon, Branston & Bayhan, 1981; Siemkowicz & Hanson, 1981). The *in vitro* rat hippocampus shows marked sensitivity to anoxia and 10 min of superfusion with anoxic buffer leads to an irreversible loss of synaptic transmission without affecting propagation of the impulse presynaptically (Kass & Lipton, 1982). Development of this irreversible, or long-term, transmission failure appears to be dependent upon the presence of normal extracellular Ca^{2+} concentrations (Kass & Lipton, 1982). The

present work examines the role played by extracellular Ca^{2+} in leading to this lesion in two different regions of the hippocampal slice, the CA1 and the dentate gyrus, notable for their marked differences in sensitivity to irreversible anoxic damage *in vivo* (Pulsinelli *et al.* 1982).

METHODS

Much of the methodology has been described elsewhere (Kass & Lipton, 1982). Hippocampi were dissected from white male rats, aged 110–130 days, and were placed on nylon-mesh grids. For electrophysiological studies slices were superfused by buffer in a circulating chamber at about 70 ml/min (Lipton & Whittingham, 1979) and for metabolic studies the slices were placed in a vial in which the buffer was vigorously bubbled either with 95 % O_2–5 % CO_2 (normoxia) or with 95 % N_2–5 % CO_2 (anoxia). In all cases the slices were positioned on nylon bolting-cloth grids (Lipton & Whittingham, 1979). Unless otherwise stated, buffer composition was (mM): NaCl, 126; KCl, 3; KH_2PO_4, 1·4; $MgSO_4$, 1·3; $CaCl_2$, 2·4; $NaHCO_3$, 26; glucose, 4; pH 7·4 at 37 ± 1 °C. This is termed 'normal buffer'. Other buffers were as the normal buffer with the following exceptions: 0 Ca^{2+}–10 mM-Mg^{2+} buffer contained 0 $CaCl_2$ and 9 mM-$MgCl_2$. Cobalt-containing buffer had 2 mM-$CoCl_2$ and 0 KH_2PO_4. KH_2PO_4 was removed from the buffer to prevent precipitation of the cobalt. We tested the effect of phosphate removal from normal buffer and it did not alter transmission or $^{45}Ca^{2+}$ uptake.

Extracellular responses to perforant path stimulation were recorded in the dentate granule cell layer and responses to Schaeffer collateral stimulation were recorded in the CA1 stratum radiatum. These electrophysiological responses were quantitated by measuring the heights of the population spikes in the two regions (Kass & Lipton, 1982).

For all biochemical and $^{45}Ca^{2+}$-uptake studies, tissue was frozen in liquid N_2, lyophilized and then weighed (dry wt.). A Mettler micro-balance was used. In many cases tissue was dissected prior to being weighed. The dissection provided a 'dentate' region and a CAl region. The former included about one half of the dentate granule cells and the molecular layer of the dentate gyrus. The latter included the region from the stratum radiatum to the alveus including the CA1 pyramidal cell layer. High-energy nucleotides were measured using the firefly luciferin–luciferase assay (Lust, Feussner, Barbehenn & Passonneau, 1982).

Calcium-uptake studies

Differentiating intracellular from extracellular $^{45}Ca^{2+}$. Ca^{2+} uptake was measured by incubating the tissue with $^{45}Ca^{2+}$, the radiolabelled tracer. Intracellular $^{45}Ca^{2+}$ was differentiated from extracellular $^{45}Ca^{2+}$ by then washing the tissue in ice-cold $LaCl_3$-fortified buffer to eliminate the extracellular tracer (Hellman, 1978). We determined the washing regime necessary to do this in experiments whose results are presented in Fig. 1. The ice-cold wash-out of $^{45}Ca^{2+}$ from the tissue can be resolved graphically into two components; these are shown in the Figure. The rapid, presumed extracellular, component has an efflux half-time of 3–4 min. The slow, presumed intracellular, phase has a half-time of about 2 h in these ice-cold conditions. These half-times ($t_{\frac{1}{2}}$) are independent of the loading time for $^{45}Ca^{2+}$. The analysis leads to the following actual values for the different pools.

For 3 min loading: rapid component, $t_{\frac{1}{2}} = 3{\cdot}3$ min, size is 0·65 nmol/mg wet wt.; slow component, $t_{\frac{1}{2}} = 123$ min, size is 0·47 nmol/mg wet wt.

For 40 min loading: rapid component, $t_{\frac{1}{2}} = 4{\cdot}3$ min, size is 0·90 nmol/mg wet wt.; slow component, $t_{\frac{1}{2}} = 115$ min, size = 2 nmol/mg wet wt.

In these, and all experiments, tissue $^{45}Ca^{2+}$ was converted to tissue Ca^{2+} by assuming the specific activity of Ca^{2+} entering the tissue is the same as the specific activity of the extracellular Ca^{2+}. The results show that after a 60 min wash-out period more than 98 % of remaining tissue $^{45}Ca^{2+}$ is 'intracellular', for tissue loaded for either 3 min or 40 min.

Thus, in all experiments we washed the $^{45}Ca^{2+}$-loaded tissue in ice-cold $LaCl_3$-fortified buffer for 60 min. Tissue was then assayed for $^{45}Ca^{2+}$ after lyophilization and dissection as described above.

Measurement of $^{45}Ca^{2+}$ uptake. $^{45}Ca^{2+}$ uptake was measured by exposing the slices to the labelled Ca^{2+} for different durations and then washing for 60 min as described above. In any one experiment, pooled slices from two hippocampi were used for the eight time points. Slices were then lyophilized, dissected, and weighed before being analysed for $^{45}Ca^{2+}$. Uptake was expressed as moles Ca^{2+} taken

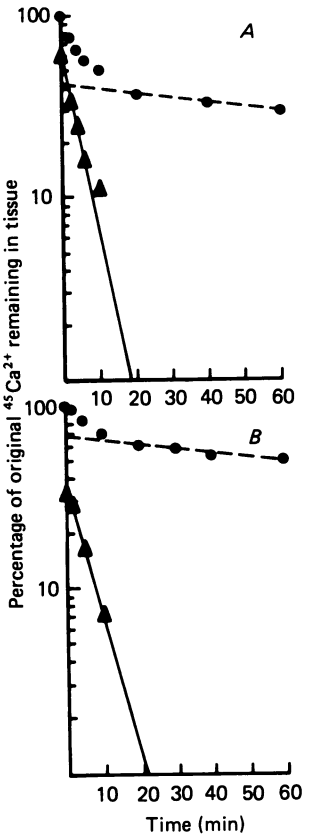

Fig. 1. $^{45}Ca^{2+}$ efflux from hippocampal slices. The slices were incubated in normal buffer and were exposed to $^{45}Ca^{2+}$ (5 μCi/ml) for either 3 (A) or 40 (B) min. They were removed, washed for 15 s in ice-cold normal buffer and then immersed in modified buffer containing 2 mM-$LaCl_3$, 0 phosphate and 0 bicarbonate at 2 °C for the periods of time indicated by the circles. At the times shown by these points, slices were removed from the modified buffer, blotted, weighed and analysed for $^{45}Ca^{2+}$. All points are averages of four experimental samples and S.E. of means are less than 7% in all cases. The circles represent the original data points and the triangles are derived by subtracting the dashed line from these original data points. At $t = 0$ min total tissue Ca^{2+} for $A = 1{\cdot}12$ nmol/mg wet wt. and $B = 2{\cdot}90$ nmol/mg wet wt.

up per tissue dry weight. In some experimental paradigms $^{45}Ca^{2+}$ uptake was measured at only one time point.

Analysis of $^{45}Ca^{2+}$ uptake curve. The resulting curve of $^{45}Ca^{2+}$ uptake *vs.* time was analysed by a non-linear regression analysis (NREG 77, Tutsch, Madison Area Computing Center) using all the points from between eight and twelve experiments. The best fit to the exponential relationship:

$$Ca_T = A_1 (1-\exp[-K_1 t]) + A_2 (1-\exp[-K_2 t]) \quad (1)$$

was determined. This equation has been applied to $^{45}Ca^{2+}$ uptake into a variety of tissues including smooth muscle (Scheid & Fay, 1984), liver cells (Barritt, Parker & Wadsworth, 1981) and cultured kidney cells (Borle, 1970). In the derivation, $^{45}Ca^{2+}$ uptake is assumed to take place from an effectively infinite pool into two exchangeable cellular pools whose sizes are A_1 and A_2 and whose first-order efflux rate constants are K_1 and K_2 (Borle, 1975). Ca_T is the total Ca^{2+} taken up at time t. For the equation to be valid the pools must either be in parallel or be in series with their rate constants differing by at least 5-fold. In this model the unidirectional influx rate into any pool, J, is equal to the efflux at the steady state; thus it is equal to $K \times A$ (Borle, 1975).

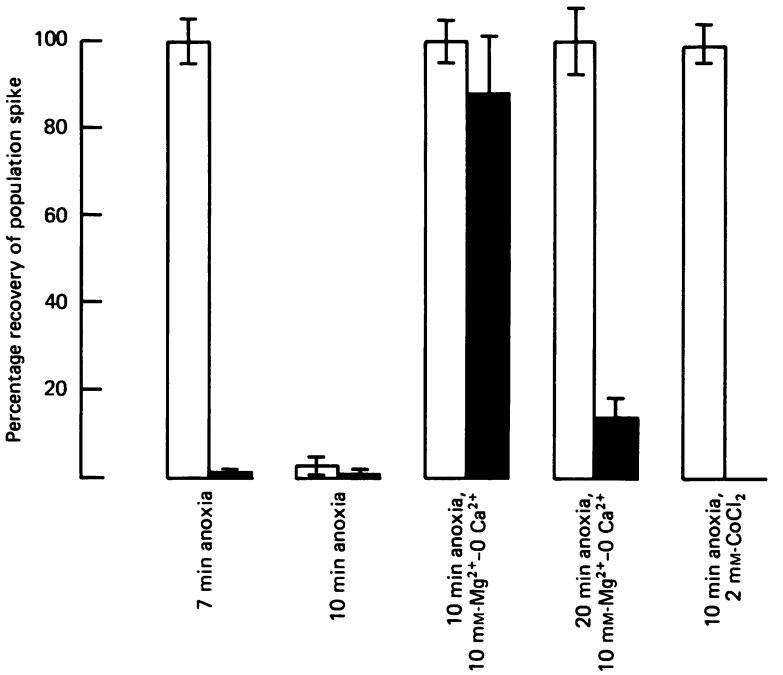

Fig. 2. Recovery of the population spike after anoxia in different incubation media. Open bars denote transmission to the dentate gyrus; filled bars denote transmission to CA1. Slices were exposed to anoxia for the durations shown. During, and for 5 min preceding and following anoxia, the buffers were either normal or were altered as indicated in the Figure. The ordinate is the average height of the population spike measured 60 min after the end of the anoxia as a percentage of the height prior to the anoxia. In all cases, bars are averages from five or more experiments ± S.E. of mean bars.

RESULTS

Effects of different buffer compositions during anoxia on the recovery of transmission

We previously showed that long-term transmission damage between the perforant path and the dentate granule cells was markedly attenuated if the buffer during anoxia contained 0 Ca^{2+}–10 mM-Mg^{2+} (Kass & Lipton, 1982). The relationship between the presence of extracellular Ca^{2+} and the degree of transmission damage was explored further and the results are shown in Fig. 2, which demonstrates the effects of maintaining varied buffer compositions during, and for 5 min before and after, an anoxic episode. In the dentate gyrus, 0 Ca^{2+}–10 mM-Mg^{2+} buffer completely protects transmission against up to 20 min of anoxia. Including 2 mM-cobalt, in the presence of normal Ca^{2+} and Mg^{2+} concentrations, completely protects transmission against 10 min of anoxia. (Longer periods were not tried because of potentially toxic effects of the cobalt.) Thus, two situations which should attenuate the entry of Ca^{2+} into the cells, exerted marked protective effects against anoxic damage.

Including the protease inhibitor leupeptin, or the phospholipase A_2 inhibitor, mepacrine, did not protect significantly against transmission damage. These results are not shown in the Figure. Recovery of the response following 1 h pre-treatment

with 40 μg mepacrine/ml and 10 min anoxia was $16 \pm 9\%$ ($n = 8$ experiments). Recovery of the response following 4 h pre-treatment with 100 μg leupeptin/ml and 10 min anoxia was $0 \pm 2\%$ ($n = 4$ experiments).

CA1 pyramidal cells are more vulnerable to irreversible anoxic morphological damage than are dentate granule cells (Pulsinelli *et al.* 1982). We determined whether they show increased susceptibility to transmission damage by comparing effects of anoxia on recovery of transmission in CA1 and the dentate gyrus. The results are

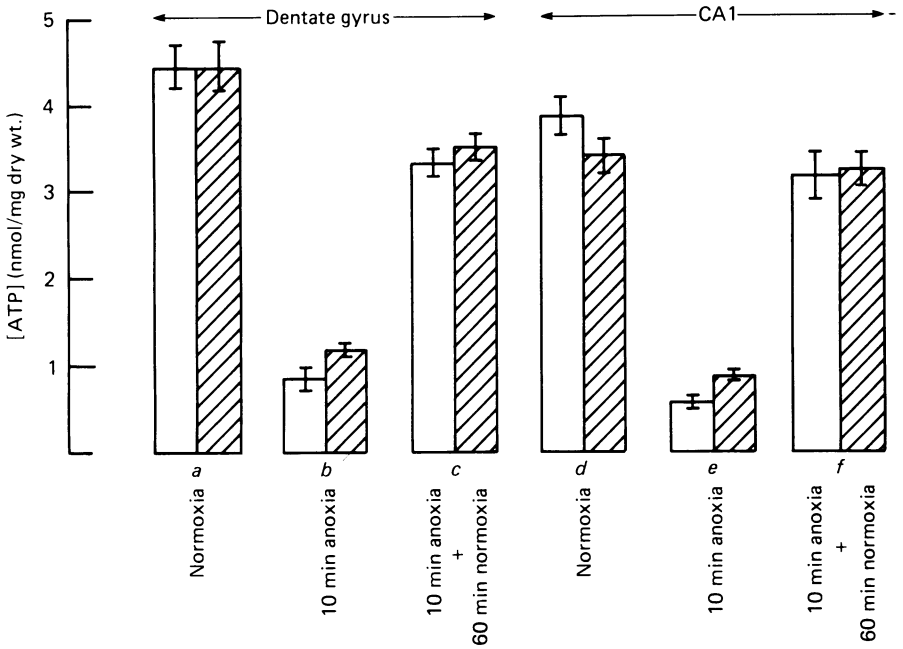

Fig. 3. ATP concentrations during and 1 h following anoxia in the dentate gyrus and CA1 regions of the slice. Open bars denote ATP concentrations in slices maintained in normal buffer throughout the experiment. The hatched bars denote slices exposed to 10 mM-Mg^{2+}–0 Ca^{2+} either for 20 min during normoxia (*a* and *d*) or during and for 5 min either side of anoxia (*b*, *c*, *e* and *f*). Slices were removed from the buffer for analysis after 3 h of normoxia (*a* and *d*), or after 3 h normoxia and 10 min of anoxia (*b* and *e*) or after 2 h normoxia and 10 min of anoxia, followed by 1 h of normoxia (*c* and *f*). All values are means from fifteen or sixteen tissue samples ($\pm$S.E. of mean).

also shown in Fig. 2, by the filled bars. It is apparent that transmission to CA1 is damaged by shorter exposures to anoxia than is transmission to the dentate gyrus. This is true both in normal buffer, where CA1 is vulnerable to 7 min of anoxia, and also in 0 Ca^{2+}–10 mM-Mg^{2+} buffer where CA1 is vulnerable to 20 min of anoxia.

Effects of anoxia, in the presence and absence of Ca^{2+}, on adenosine 5′-triphosphate (ATP) levels in CA1 and the dentate gyrus

We measured the changes in tissue ATP levels in CA1 and the dentate gyrus, at the end of a 10 min anoxic period and also 1 h after the resumption of normoxic perfusion. These studies were done on tissue which was exposed to normal buffer during anoxia and also on tissue which was exposed to 0 Ca^{2+}–10 mM-Mg^{2+} buffer during the anoxia.

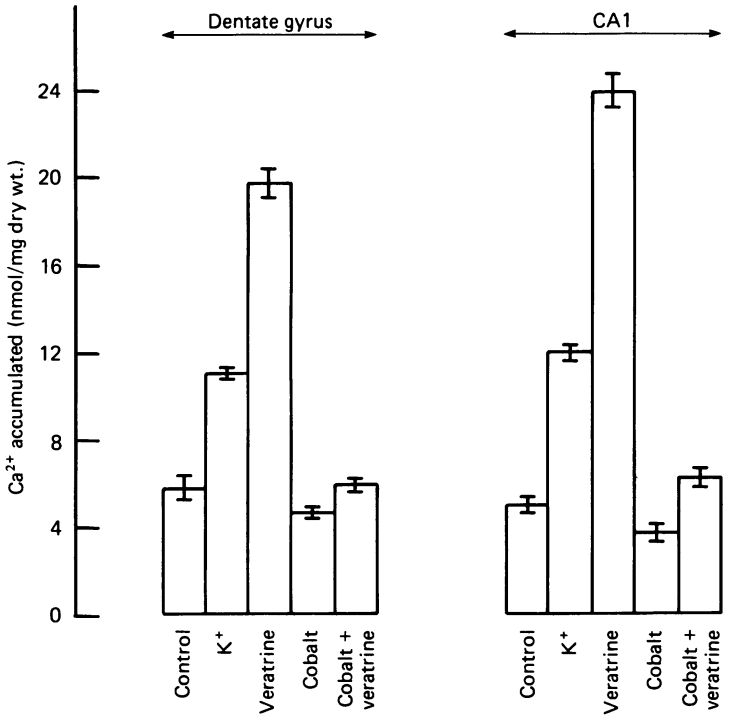

Fig. 4. Effects of depolarizing agents on $^{45}Ca^{2+}$ uptake. Slices were exposed to $^{45}Ca^{2+}$ (5 μCi/ml) for 10 min in one of the following conditions: normal buffer (control); buffer containing 60 mM-K^+, isosmotically substituted for Na^+; buffer containing 50 μM-veratrine; buffer containing 2 mM-cobalt and no phosphate; buffer containing 2 mM-cobalt, veratrine and no phosphate. The bars represent the $^{45}Ca^{2+}$ uptakes during the 10 min periods (±S.E. of means) and are averages from between eight to twelve experiments. Excluding phosphate did not affect $^{45}Ca^{2+}$ uptake in normal buffer; nor did it affect the veratrine-stimulated $^{45}Ca^{2+}$ uptake.

The experiments had two distinct purposes. The first was to determine whether the increased anoxic sensitivity of transmission in the CA1 region was associated with a more profound fall in ATP in that region than in the dentate gyrus during the anoxia. The second purpose was to determine whether the protection against transmission damage which occurred in 0 Ca^{2+}–10 mM-Mg^{2+} buffer was associated with an attentuation in the fall of ATP, either during or following anoxia. The results are shown in Fig. 3. Regarding the first issue it is apparent that in normal-Ca^{2+} buffer the percentage decrease in ATP during anoxia is very similar in the dentate gyrus and CA1; the decrease in the dentate gyrus is to 18% of control values while in CA1, ATP decreases to 15% of control values. The difference in basal levels of ATP between the two regions is not readily interpretable as the two samples include quite different tissue components. Regarding the second point; decreasing the extracellular Ca^{2+}–Mg^{2+} ratio does somewhat attenuate the fall in ATP during anoxia. The fall in CA1 is decreased from an 85% drop to a 75% drop. The difference is significant at $P < 0{\cdot}01$ using the Student's t test. While the drop in the dentate gyrus is decreased from 80% to 75%, this difference is not significant ($P > 0{\cdot}05$).

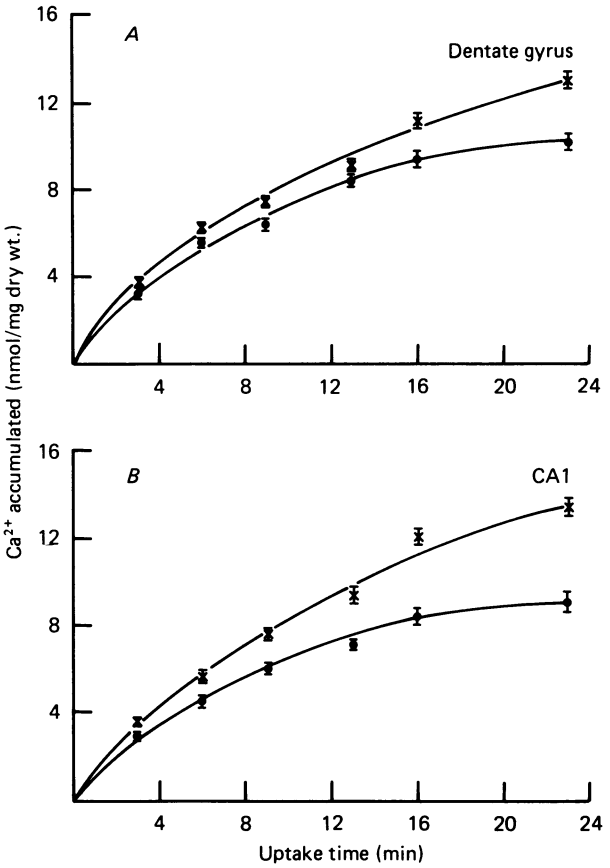

Fig. 5. Uptake of $^{45}Ca^{2+}$ by the dentate gyrus and CA1 regions of the slice during anoxia and normoxia. For normoxia (circles) slices were exposed to $^{45}Ca^{2+}$ for the times indicated by the circles and tissue was then removed for analysis. For anoxia (crosses), slices were exposed to N_2–CO_2 for 7 min; the $^{45}Ca^{2+}$ was then added to this anoxic buffer and the exposure continued for the same durations as the normoxic cases. Points are averages from eight or nine experimental observations, bars are S.E. of means. Curves are drawn by eye.

Ca^{2+} accumulation

Effects of depolarizing agents. In order to verify whether the 'lanthanum-wash' procedure measured cellular Ca^{2+} accumulation in this preparation, we measured the effects of two agents which have been widely shown to increase Ca^{2+} uptake in excitable tissues: veratrine and elevated extracellular K^+. The results are shown in Fig. 4. It is apparent that veratrine increases the 10 min uptake of $^{45}Ca^{2+}$ by 3- to 4-fold; 60 mM-K^+ increases uptake by about 2·5-fold. The drug-induced increase is almost completely blocked by 2 mM-cobalt. Thus, the method does appear to measure changes in intracellular $^{45}Ca^{2+}$. It is notable that the percentage increase in uptake is greater in CA1 than in the dentate gyrus for both agents. For veratrine this regional difference is significant at $P < 0{\cdot}001$ and for high K^+, it is significant at $P < 0{\cdot}02$, using the Student's t test.

TABLE 1. Kinetic constants for $^{45}Ca^{2+}$ uptake into the dentate gyrus and CA1 ± anoxia

	Dentate gyrus		CA1	
Constant	Control	Anoxia	Control	Anoxia
A_1: total exchangeable Ca^{2+} (nmol/mg dry wt.)	11·5* ±0·5	14·9* ±0·8	10·0* ±0·4	17·7* ±1·3
K_1: efflux rate constant (/min)	0·103† ±0·010	0·083† ±0·008	0·103* ±0·009	0·064* ±0·008
J_{12}: unidirectional influx rate (nmol/mg dry wt. . min)	1·15	1·19	1·00	1·06
$t_{\frac{1}{2}}$: turnover half-time (min)	6·9	8·7	6·9	11·6

A_1 is the total exchangeable Ca^{2+}; K_1 is the efflux rate constant. J_{12}, the unidirectional influx rate, is calculated as $K_1 \times A_1$. $t_{\frac{1}{2}}$ is the half-time for accumulation of $^{45}Ca^{2+}$ into the exchangeable pool, and is equal to $\ln 2/K_1$. Values are averages ± S.E. of mean calculated using a non-linear regression programme to fit the data in Fig. 5 to the eqn. (1). The data are best fitted by the mono-exponential relationship $Ca_T = A_1 (1 - \exp(-K_1 t))$ where Ca_T is Ca^{2+} taken up after t min. Significance of differences: *, $P < 0·01$; †, $P < 0·05$.

Effects of anoxia on Ca^{2+} uptake. The results of these studies are shown in Fig. 5. $^{45}Ca^{2+}$ uptake was measured as a function of time of exposure to the radiolabelled tracer for slices in anoxic buffer, and for slices in normoxic buffer. The anoxic $^{45}Ca^{2+}$ uptake was measured on slices which were anoxic for 7 min prior to the addition of $^{45}Ca^{2+}$ and for up to a further 23 min. This was done to provide as near as possible steady-state conditions during the $^{45}Ca^{2+}$ uptake (see below).

Three aspects of the results are notable. (1) Uptake of $^{45}Ca^{2+}$ during anoxia is increased in both the dentate gyrus and CA1 regions of the slice; (2) this increased uptake is larger in CA1 than in the dentate gyrus and (3) the percentage effect of anoxia on uptake increases with increasing uptake times. The latter suggests that anoxia is augmenting uptake primarily by decreasing efflux rather than by increasing influx (Borle, 1975) and this suggestion appears to be borne out by the kinetic analysis of the curves which is shown in Table 1. Attempts were made to fit the uptake curves to the two-term exponential expression described in the Methods (eqn. (1)). However, the best fit, in all four cases, was obtained using a one-term exponential to describe the uptake. This shows that uptake may be considered to be taking place into one kinetically homogenous compartment. The analysis of the uptake curves, in Table 1, shows that anoxia increases total exchangeable Ca^{2+} by 30% in the dentate gyrus and by 77% in CA1. This increase is completely accounted for by a decrease in the efflux rate constant in both these regions; the decrease is 19% in the dentate gyrus and 38% in CA1. Thus, inhibition of Ca^{2+} efflux processes is twice as great in CA1 as it is in the dentate gyrus. Anoxia has no significant effect on J, the calculated unidirectional influx rate, in either region. Fig. 6 shows the fit of the data, for CA1, to the curve derived from the constants in Table 1. The fit is good except for the 3 min data points which are higher than the calculated points. (This is also true for the dentate gyrus region, not shown.)

The reliability of the above kinetic analysis depends on the Ca^{2+}-transport properties of the tissue not varying greatly during the measurements. For example,

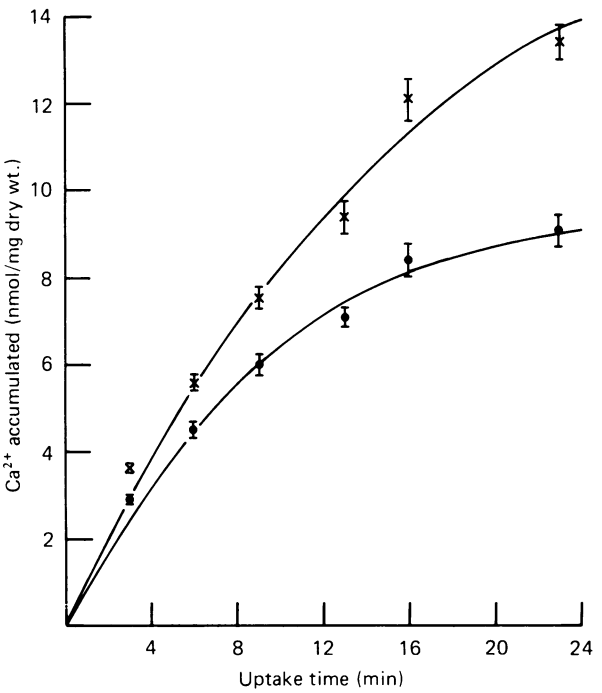

Fig. 6. Fit of uptake data in Fig. 5*B* to the exponential function derived from the kinetic analysis in Table 1. The points are the observations shown in Fig. 5*B* for CA1. The curves are the exponential functions derived from the constants shown in Table 1. Circles, normoxia; crosses, anoxia.

the observed effect of anoxia could be explained if the unidirectional uptake of $^{45}Ca^{2+}$ was gradually increasing during the 23 min of anoxia in which the $^{45}Ca^{2+}$ was present; this also would produce an anoxic curve in which the anoxic uptake became progressively greater than the normoxic uptake. Table 2A, shows that the unidirectional uptake rate did not change during the course of the exposure to anoxia. Thus uptake during 3 min, which is largely determined by the unidirectional influx (Borle, 1975), is unchanged between 7 and 30 min of anoxia. It is notable, too, that 3 min uptake is not significantly augmented by anoxia. It was also important to determine whether the net uptake kinetics were varying between 7 and 30 min. Uptake was measured during 10 min periods beginning at different times during the anoxia. We reasoned that if effects of anoxia on the efflux became greater with longer anoxic exposure then this would be manifested by larger effects of anoxia on 10 min uptake as the duration of exposure to anoxia increased. The results of these studies are shown in Table 2 B. By 7 min, the time at which the kinetic measurements were begun, $^{45}Ca^{2+}$ uptake during 10 min is approximately 90% of its maximal value for both regions. Thus, the uptake kinetics appear to be quite, although not completely, steady between 7 and 30 min of anoxia. In our analysis we assume that the kinetic parameters are constant during this interval.

Effects of cobalt and creatine on $^{45}Ca^{2+}$ uptake. Both cobalt (Fig. 2) and pre-incubation with 25 mM-creatine (Kass & Lipton, 1982) protect transmission in the dentate gyrus

TABLE 2. $^{45}Ca^{2+}$ uptake by the dentate gyrus and CA1 regions of the hippocampal slice at different times during anoxia. In all cases, slices were incubated for 2·0–2·5 h before $^{45}Ca^{2+}$ was added. $^{45}Ca^{2+}$ was added at the time shown, in minutes, after the slices were moved to the anoxic buffer. For −values, measurements were made in normoxia throughout

A, uptake for 3 min periods begun at various times during 30 min exposure to anoxia

Time after (or before (−)) onset of anoxia at which $^{45}Ca^{2+}$ is added (min)	Uptake of $^{45}Ca^{2+}$ during 3 min* (nmol/mg dry wt.)	
	CA1	Dentate gyrus
−3	2·99 ± 0·22	4·20 ± 0·24
7	3·30 ± 0·08	3·79 ± 0·22
17	2·81 ± 0·30	3·82 ± 0·16
27	3·37 ± 0·33	3·74 ± 0·18

* Values are means ± S.E. of mean of eight experimental samples.

B, uptake for 10 min periods begun at various points during 30 min exposure to anoxia

Time after (or before (−)) onset of anoxia at which $^{45}Ca^{2+}$ is added (min)	Uptake of $^{45}Ca^{2+}$ during 10 min* (nmol/mg dry wt.)	
	CA1	Dentate gyrus
−10	5·63 ± 0·25	6·69 ± 0·36
0	7·00 ± 0·37	7·87 ± 0·69
3	8·38 ± 0·35	8·52 ± 0·57
7	9·09 ± 0·48†	8·26 ± 0·36‡
13	9·60 ± 0·24	8·57 ± 0·41
20	10·14 ± 0·26†	9·19 ± 0·34‡

* Values are means ± S.E. of mean of nine samples. Significance of differences: †, $P < 0·025$; ‡, $P < 0·025$.

against irreversible anoxic damage. If Ca^{2+} entry is associated with transmission damage, then the above protective effects might well be associated with a diminution of Ca^{2+} entry during anoxia. Fig. 7 shows the effect of including 2 mM-cobalt in the incubation medium on $^{45}Ca^{2+}$ uptake during anoxia.

Cobalt lowers the normoxic $^{45}Ca^{2+}$ uptake by 20 % in both the dentate gyrus and CA1. However, in the dentate gyrus the absolute rise in $^{45}Ca^{2+}$ uptake during anoxia is the same whether or not cobalt is present. In CA1, cobalt slightly attenuates the anoxic increase in $^{45}Ca^{2+}$ uptake (by 17 %). In neither region is anoxic $^{45}Ca^{2+}$ uptake in the presence of cobalt greater than normoxic uptake in the absence of cobalt.

Fig. 8 shows the effects of pre-incubating the slices for 2 h in 25 mM-creatine, on $^{45}Ca^{2+}$ uptake during anoxia. It has been shown previously that creatine pre-incubation elevates cell phosphocreatine substantially so that, during anoxia, the fall in ATP and the increase in cell Na^+–K^+ ratio is markedly attenuated. Along with this there is an approximate 80 % protection against anoxic transmission loss in the dentate gyrus (Kass & Lipton, 1982) and a 50 % protection in CA1 (Kass & Lipton, 1983). While creatine pre-incubation has no effect on normoxic $^{45}Ca^{2+}$ uptake, it markedly attenuates the anoxic increase. This attenuation is 40 % in the dentate gyrus and 60 % in CA1. The data in Figs. 7 and 8, then, show that two treatments which protect transmission against damage also markedly reduce the net $^{45}Ca^{2+}$ uptake during anoxia.

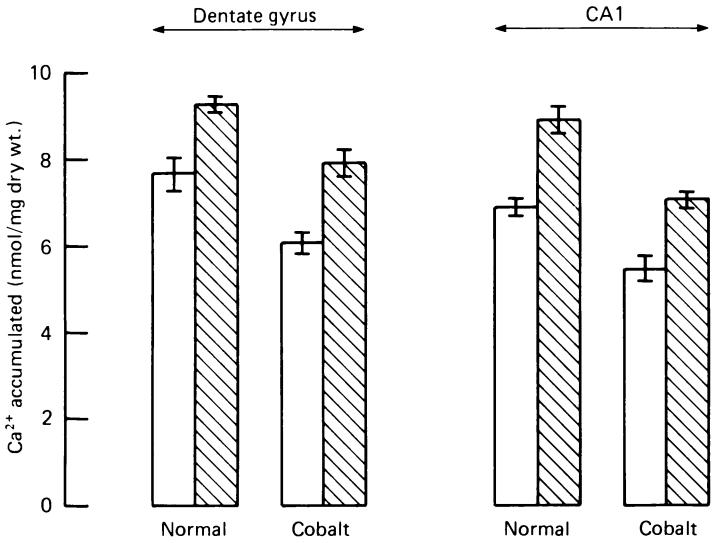

Fig. 7. Effect of 2 mM-cobalt on $^{45}Ca^{2+}$ uptake during normoxia and anoxia. The open bars denote $^{45}Ca^{2+}$ uptake during normoxia and the hatched bars denote $^{45}Ca^{2+}$ uptake during anoxia. $^{45}Ca^{2+}$ uptake was measured for 10 min, either during normoxia or between 7 and 17 min of anoxia. For cobalt, slices were transferred to a normal buffer without phosphate and containing 2 mM-cobalt chloride 7 min before, and all during, the exposure to $^{45}Ca^{2+}$. Bars are averages of eight or nine experimental observations, ±S.E. of means. All differences between normoxia and anoxia are significant with $P < 0{\cdot}001$; all differences between cobalt and control, during normoxia, are also significant at $P < 0{\cdot}001$. Differences between effects of anoxia with and without cobalt are not significant ($P < 0{\cdot}2$).

Effect of ouabain on $^{45}Ca^{2+}$ uptake. The kinetic analysis of the uptake data, in Table 1, suggested that the major effect of anoxia on Ca^{2+} uptake was exerted via an inhibition of Ca^{2+} efflux. The two major modes of Ca^{2+} efflux in brain tissue appear to be the Na^+-gradient-driven Na^+–Ca^{2+} exchange mechanism and the ATP-driven Ca^{2+} pump (Gill, Grollman & Kohn, 1981). During anoxia in these hippocampal slices intracellular Na^+ is increased from 73 to 132 mM and intracellular K^+ is reduced from 113 to 56 mM (Kass & Lipton, 1982). 1×10^{-6} M-ouabain produces an almost identical change in these cations and 3×10^{-6} M-ouabain causes an even larger change (Kass & Lipton, 1982). We examined the effects of these concentrations of ouabain on $^{45}Ca^{2+}$ uptake to determine if inhibition of Na^+–Ca^{2+} exchange might be accounting for the anoxic accumulation of Ca^{2+}. The results are shown in Table 3; it is apparent that even 3×10^{-6} M-ouabain has no effect on 23 min Ca^{2+} uptake, in either the dentate gyrus or CA1.

DISCUSSION

The results demonstrate three major points. First, there is an increased accumulation of radiolabelled Ca^{2+} in both CA1 and dentate gyrus regions of the hippocampal slice during anoxia. This appears to result largely from inhibition of Ca^{2+} efflux across the plasmalemma of neurones; the Na^+-gradient-driven Ca^{2+}-extrusion mechanism

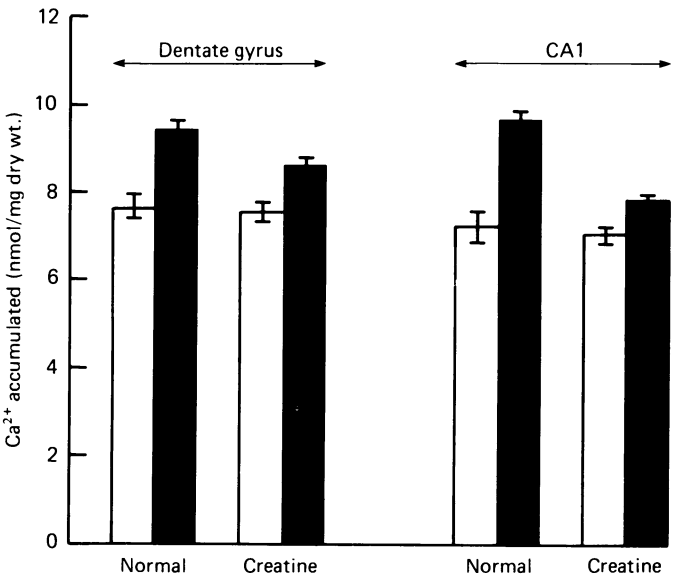

Fig. 8. Effect of 25 mM-creatine pre-incubation on $^{45}Ca^{2+}$ uptake during normoxia and anoxia. The open bars denote $^{45}Ca^{2+}$ uptake during normoxia and the filled bars denote $^{45}Ca^{2+}$ uptake during anoxia. $^{45}Ca^{2+}$ uptake was measured for 13 min either during normoxia or between 7 and 20 min of anoxia. For creatine, slices were incubated in buffer containing 25 mM-creatine for 2 h and then were returned to normal buffer for 30 min before beginning the anoxia and the $^{45}Ca^{2+}$ uptake. Bars are averages from nine experiments ±S.E. of means. For the dentate gyrus the difference in the anoxic increase in $^{45}Ca^{2+}$ uptake between control- and creatine-treated tissues is significant at $P < 0.1$; for CA1 this difference is significant at $P < 0.005$, using Student's t test. All effects of anoxia are significant at $P < 0.05$ or $P < 0.01$.

TABLE 3. Effect of ouabain on $^{45}Ca^{2+}$ uptake

	$^{45}Ca^{2+}$ uptake (nmol/mg dry wt.)	
[Ouabain] (M)	Dentate gyrus	CA1
0	11·5±0·4	10·0±0·5
1×10^{-6}	12·6±0·4	11·0±0·6
3×10^{-6}	11·7±0·5	10·8±0·5

Rat hippocampal slices were exposed to ouabain at the designated concentrations for 70 min. During the final 23 min they were also exposed to $^{45}Ca^{2+}$. Each value is the mean of eight independent observations ±S.E. of mean. There are no significant differences ($P < 0.05$) between any of the values in a column.

is not the process which is inhibited. Secondly, long-term anoxic damage to synaptic transmission is strongly reduced when conditions are established which reduce the excess accumulation of Ca^{2+} during anoxia. Thirdly, transmission through CA1 is vulnerable to shorter periods of anoxia than is transmission through the dentate gyrus and, perhaps relatedly, the anoxic accumulation of Ca^{2+} in CA1 is about twice that in the dentate gyrus. The results are most simply interpreted to show that

long-term damage results from a net cellular accumulation of Ca^{2+} during and (possibly) shortly after anoxia; that the increased sensitivity in CA1 results from a larger 'anoxic' Ca^{2+} accumulation in that region, and, finally, that this 'anoxic' Ca^{2+} accumulation occurs as a result of inhibition of the ATP-driven Ca^{2+}-extrusion pump across the neuronal plasmalemma following the fall in ATP which occurs during anoxia. The data in no way exclude the possibility that a factor in addition to Ca^{2+} accumulation is also necessary to produce the long-term damage.

Several groups have suggested that increased cytosolic Ca^{2+} is a trigger for irreversible anoxic or ischaemic brain damage (Haas, 1981; Meldrum, 1981; Siesjo, 1981). However, the only direct evidence comes from studies on the *in vitro* retina. In that tissue omission of Ca^{2+} during anoxia partially blocks the development of irreversible deficits in rates of protein synthesis (Ames & Nesbett, 1983). The present results thus are important as they do provide direct evidence associating long-term anoxic damage with Ca^{2+} entry in brain tissue.

Kinetic analysis of Ca^{2+} accumulation

We used an ice-cold La^{3+} wash to eliminate extracellular $^{45}Ca^{2+}$ and concluded that the $^{45}Ca^{2+}$ remaining in the tissue after this wash was intracellular. The evidence for this includes the following: (i) the ice-cold wash-out curve (Fig. 1) has two components. The size and rate constant of the fast component suggest it is extracellular. Its wash-out half-time in the cold, of a few minutes, is similar to that of other, presumed extracellular, markers (Lipton & Heimbach, 1977; Lipton & Heimbach, 1978; Amtorp, 1979); (ii) inclusion of La^{3+} during a wash-out, (Van Breemen, Farinas, Casteels, Greba, Wuttack & Deth, 1973) particularly in the cold (Hellman, 1978), has been shown to allow release of extracellular and membrane-bound Ca^{2+} while not allowing significant release of intracellular Ca^{2+}; (iii) the postulated intracellular pool is greatly augmented by veratrine and by high K^+, two agents thought to increase intracellular Ca^{2+} in brain tissue (e.g. Szerb, Ross & Gurevich, 1981).

Uptake of $^{45}Ca^{2+}$ into many cells can be described as a mono-exponential function of time (Borle, 1969; Borle, 1970). The simplest interpretation of the mono-exponential uptake is that the bulk of the $^{45}Ca^{2+}$ accumulation during an uptake experiment is into one kinetically homogenous pool (Borle, 1969). Thus, there appears to be one major kinetically homogenous intracellular pool in each of the CA1 and dentate gyrus regions of these hippocampal slices. (The data hinted that there may also be a small rapidly turning-over pool such as that observed in liver by Barritt *et al.* (1981) because the mono-exponential curve underestimated the actual uptake at the earliest, 3 min, time point.) The properties of each of those major pools are shown in Table 1. The calculated pool size of about 10 nmol/mg dry wt. is about twice that observed for whole pituitary slices (Moriarty, 1980) and whole hippocampal slices (Baimbridge & Miller, 1981); accumulation in neuropil may well be higher than in tissue as a whole. If one assumes that cell water is four times cell dry weight (an average value from many observations we have made), and that the uptake occurs into cylindrical neuronal elements whose diameter is 2 μm then the calculated resting influx, J_{12}, is equal to about 0·16 pmol/cm^2 . s. This is about 60 % greater than measured influx rates across the plasmalemma of the squid giant axon in physiological conditions (DiPolo,

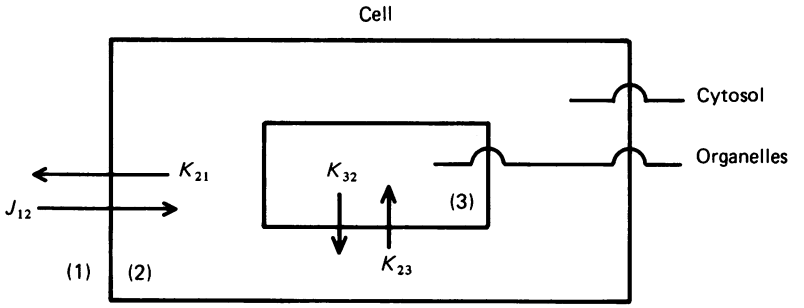

Fig. 9. Model of cell after Scheid & Fay (1984); (1) is the extracellular space. Intracellular Ca^{2+} is considered to be distributed between the organelle pool (3) and the cytosolic pool (2). Each of these is kinetically homogenous, that is, transport into and out of each pool may be described by two rate constants. K_{21}, K_{23} and K_{32} are those rate constants; J_{12} is the undirectional rate of influx into the cell at the normal extracellular Ca^{2+} concentration.

1979). The turnover half-times, calculated from the efflux rate constants, are very similar to half-times calculated for liver cells (Barritt *et al.* 1981) and brain cortex slices (Stahl & Swanson, 1972).

While the above analysis, using eqn. (1), is commonly used it ignores the quite well-established fact that intracellular Ca^{2+} is segregated into a very small cytosolic pool and a far larger organelle pool (Moriarty, 1980; Perney, Dinerstein & Miller, 1984). Scheid & Fay (1984) have analysed Ca^{2+} uptake into a model cell in which two such Ca^{2+} pools are considered. This model is shown in Fig. 9 and while Scheid & Fay demonstrated that uptake is mono-exponential if certain conditions are met they did not present expressions relating measured constants to the parameters defined in the model. We have analysed uptake into the model cell, making a slightly different simplifying assumption from that made by Scheid & Fay. Rather than assuming that $K_{21} \ll K_{23}$ (rate constants for efflux across plasmalemma and influx into organelles, respectively), an assumption that is not explicitly supported by any data, we have only assumed that the cytosolic compartment is far smaller than the organelle compartment. Both approaches assume one kinetically homogenous organelle pool because of the mono-exponential nature of the observed uptakes. The actual analysis is in the Appendix and Ca^{2+} uptake is the following function of time:

$$Ca_t = A_T\left(1-\exp\frac{[-K_{32}K_{21}t]}{K_{21}+K_{23}}\right), \tag{2}$$

where Ca_t is the total Ca^{2+} taken up into the cell at time t and A_T is the steady-state amount of exchangeable Ca^{2+} in the cell.

Uptake of Ca^{2+} is still a mono-exponential function of time. However, the effective efflux rate constant for the one pool is not equal to K_{21} but, rather, is equal to K' in the following expression:

$$K' = \frac{K_{32}K_{21}}{K_{21}+K_{23}} \tag{3}$$

and should be considered an apparent rate constant. This is the parameter which is

calculated by the non-linear regression analysis used to assemble Table 1. Thus, it is equal to K_1 in that table. The apparent rate constant is a function of the transport processes across the organelle membranes (K_{23} and K_{32}) as well as of K_{21}, the rate constant for efflux across the plasmalemma.

This analysis does not alter the significance of the calculated parameter A_1 in Table 1; it represents total cell exchangeable Ca^{2+}. It does alter the significance of the calculated efflux rate constant. As noted above, it is no longer simply a property of the plasmalemma. It also alters the significance of the calculated unidirectional influx, J_{12}. As shown in the Appendix, this calculated value is only an approximation to the actual unidirectional influx; it becomes equal to the influx only if $K_{21} \ll K_{23}$. As mentioned above, while this is often assumed to be the case it may well not be so.

Effects of anoxia on Ca^{2+} accumulation

Anoxia significantly increases the size of the intracellular Ca^{2+} pool in each region. Making a simplifying assumption that the kinetic parameters abruptly assume their anoxic values 3 min after the onset of anoxia one can use the data in Table 1 to calculate that exchangeable Ca^{2+} will increase by 11% in the dentate gyrus and by 25% in CA1 after 10 min of anoxia. Although the data in Table 2B show that the simplifying assumption is not strictly true it does allow a reasonable estimate of the change in cell Ca^{2+} at the time that long-term damage is occurring.

Analysis of each Ca^{2+}-uptake curve reveals that the increased uptake during anoxia can be almost completely accounted for by a decrease in the calculated efflux rate constant for the intracellular pool, in both CA1 and the dentate gyrus. The analysis does assume unchanging values of the kinetic parameters during the uptake and while our studies showed that the 10 min uptake was changing, the change was only 10% during the 23 min uptake period and it did not prevent description of the uptake as a mono-exponential process, even during anoxia. Other evidence strongly suggested that the increased uptake resulted from inhibition of efflux. The 3 min uptake of $^{45}Ca^{2+}$, which does reflect unidirectional influx, is not increased at all by anoxia. The calculated values of J_{12}, in Table 1, are unchanged by anoxia and while these calculated values are not strictly equal to the unidirectional influx (see Appendix) the two are probably not very different. Finally, at concentrations which almost completely eliminate the veratrine-induced increase in Ca^{2+} uptake, cobalt does not block the increased uptake during anoxia. This strongly suggests that the anoxic uptake is not due to opening of depolarization-sensitive channels.

Eqn. (3) shows that the calculated decrease in the apparent efflux rate constant during anoxia could result from (1) a decrease in K_{21}; (2) a decrease in K_{32} or (3) an increase in K_{23}. From what we know of the effects of anoxia, (2) and (3) seem very unlikely. They would imply that anoxia either decreases the rate constant for efflux from the organelles or increases the intrinsic rate of uptake into the organelles. In fact, the opposite is expected (i.e. anoxia should decrease the uptake, which is energy dependent, and should increase the efflux from, at least, mitochondria where efflux is increased when intracellular Na^+ is increased (Crompton, Moser, Ludi & Carafoli, 1978). Thus, it appears safe to conclude from the kinetic analysis that the decrease in the measured efflux rate constant during anoxia is due to an inhibition of Ca^{2+} efflux across the plasmalemma. Indeed, because of the probable effects of anoxia on

organelle transport the actual decrease in the efflux rate constant is probably larger than the calculated decrease.

The lack of an effect of 3×10^{-6} M-ouabain on Ca^{2+} uptake, even though it dramatically increases cell Na^+ (Kass & Lipton, 1982), suggests that the Ca^{2+}–Na^+ transport system (Gill, Grollman & Kohn, 1981) is not making a significant contribution to Ca^{2+} homoeostasis in the resting cell. This conclusion was also arrived at by Snelling & Nicholls (1985) for rat brain synaptosomes. While others have reported that ouabain increases $^{45}Ca^{2+}$ uptake in brain slices (e.g. Cooke & Robinson, 1971), large doses of ouabain were used and these lowered cell ATP (our observations). The absence of an effect of ouabain on $^{45}Ca^{2+}$ uptake of course also suggests that anoxia is not decreasing Ca^{2+} efflux by inhibiting the Ca^{2+}–Na^+ exchange. Thus, by a process of elimination the data argue that inhibition of the Ca^{2+}-ATPase-driven Ca^{2+}-extrusion pump is the basis for the anoxic Ca^{2+} accumulation. Studies on synaptosomes (Snelling & Nicholls, 1985) and liver cells (Bellomo, Nicotera & Orrenius, 1984) have indicated that inhibition of this efflux system does lead to significant accumulation of tissue Ca^{2+}.

Calcium entry and long-term transmission damage

The data show a clear correlation between the amount of Ca^{2+} accumulated by the cells during anoxia and the degree of irreversible transmission damage. Creatine pre-incubation and 0 Ca^{2+}-containing buffer both limit the anoxic increase in Ca^{2+} uptake and attenuate damage. Cobalt does not alter the anoxic increase in Ca^{2+} uptake; however, it does lower basal Ca^{2+} uptake so that the anoxic increase does not elevate net uptake above its value in normoxic medium. (Interestingly, cobalt has a very similar percentage effect on basal Ca^{2+} influx in dialysed squid axon (Dipolo, 1979).) This suggests that normal transmembrane fluxes of Ca^{2+} can be well tolerated by the cells during anoxia and that leakage from intracellular organelles during anoxia does not lead to long-term transmission damage.

Neither the intracellular locus, nor the mechanism, of the Ca^{2+} toxicity are known. Our results do argue against certain possibilities. Ca^{2+} does not seem to be toxic because it is decreasing cell ATP. There is a slight attenuation of the anoxic fall in ATP in the 0 Ca^{2+} – 10 mM-Mg^{2+} buffer; however, it is far smaller than the attenuation that was produced by creatine pre-incubation in previous studies (Kass & Lipton, 1982), and that pre-incubation only protected transmission by 80% in the dentate gyrus and by 50% in CA1 (Kass & Lipton, 1982, 1983). Neither leupeptin nor mepacrine (quinacrine) protected against the damage, suggesting that neither protease nor phospholipase A_2 activations are causing the damage. However, although leupeptin does appear to enter cells and inhibit certain proteases (Libby & Goldberg, 1978; Staubli, Baudry & Lynch, 1984), and mepacrine does block phospholipase A_2 activation in certain cell types (Blackwell, Flower, Nijkamp & Vane, 1978) we do not know if the substances are effective in this preparation so that no firm conclusion can be drawn from these null effects. Recent studies suggest glutamate interaction with receptors may contribute to anoxic damage (Rothman, 1984; Simon, Swan, Griffiths & Meldrum, 1984). This could be one mediator of the action of increased cell Ca^{2+}.

Finally it is notable that the calculated increase in total cell Ca^{2+} during 10 min

of anoxia is quite small; approximately 25%. The distribution of this Ca^{2+} is not known. If it is all cytosolic then it would be an extremely large percentage increase and could well be extremely toxic. On the other hand, if organelle buffering power is not severely compromised during anoxia, and it is apparently not during exposure of brain slices to high doses of cyanide (Cooke & Robinson, 1971), then the rise in cytosolic Ca^{2+} may be quite small. In neither case will the percentage rise in organelle Ca^{2+} be very large. This raises the issue of whether or not the entering Ca^{2+}, alone, is responsible for the observed damage. In reported cases of Ca^{2+}-mediated cell toxicity, in normoxia, 2- to 3-fold increases in cell Ca^{2+} are associated with damage (e.g. Happel, Banik, Balentine & Hogan, 1984).

Differential sensitivity of the CA1 and dentate gyrus to anoxia

CA1 pyramidal cells are far more vulnerable to morphological damage from anoxia than are dentate granule cells (Pulsinelli *et al.* 1982); durations of cerebral ischaemia which cause the death of a large percentage of CA1 pyramidal cells cause no long-term damage to dentate granule cells. In the current studies anoxia increased Ca^{2+} uptake into CA1 by about twice as much as into the dentate gyrus. At the same time transmission through CA1 was irreversibly damaged by exposures to anoxia which were too short to damage transmission through the dentate gyrus. The results, then, are qualitatively consistent with a conclusion that differential accumulation of Ca^{2+} during anoxia is responsible for the differential sensitivities of transmission in the two regions. The locus of the long-term transmission damage is not known. However, if it is in the dendrites of the pyramidal cells then the high anoxic sensitivity of transmission in CA1 could reflect the same phenomenon as does the high sensitivity of morphological damage to the CA1 cells. In this regard it is notable that morphological anoxic damage in CA1 appears to originate in the cell processes (Petito & Pulsinelli, 1984).

It is not clear why the accumulation of Ca^{2+} is greater in CA1 than in the dentate gyrus. ATP does fall to a lower level during anoxia in CA1 than in the dentate gyrus but this is not due to a larger percentage fall; basal ATP levels are lower in CA1 so that the functional significance of the lower anoxic ATP is difficult to interpret. There is some depolarization-sensitive entry of Ca^{2+} into CA1 but this is not nearly enough to account for the difference between the uptakes in the two regions.

In summary, the studies demonstrate a clear correlation between the amount of Ca^{2+} accumulation and the degree of irreversible transmission damage during anoxia in this rat hippocampal slice; this correlation extends to a comparison between the two hippocampal regions, CA1 and the dentate gyrus. The more vulnerable CA1 accumulates twice as much excess Ca^{2+} during anoxia as does the dentate gyrus. The basis for the anoxic Ca^{2+} accumulation appears to be an inhibition of ATP-driven Ca^{2+} efflux.

APPENDIX

Analysis of $^{45}Ca^{2+}$ uptake vs. time into the model cell depicted in Fig. 9

Symbols: R_i is the radioactivity in the i^{th} compartment (d/min . mg tissue dry wt.).
X_i is the specific activity in the i^{th} compartment (d/min . nmol).
Ca_i is total Ca^{2+} in the i^{th} compartment (nmol/mg tissue dry wt.).
J_{ij} is the flux of Ca^{2+} from the i^{th} to the j^{th} compartment (nmol/mg tissue dry wt . min).

Other symbols are as shown in Fig. 9. (These symbols are those used by Borle (1969) except that J rather than ϕ is used for flux.)

By definition: $$\frac{dR_{2+3}}{dt} = J_{12}X_1 - J_{21}X_2. \tag{A1}$$

By definition: $$J_{21} = Ca_2 K_{21} \quad \text{and} \quad X_2 = \frac{R_2}{Ca_2}. \tag{A2}$$

Therefore: $$\frac{dR_{2+3}}{dt} = J_{12}X_1 - K_{21}R_2. \tag{A3}$$

By definition: $$\frac{dR_2}{dt} = J_{12}X_1 - K_{21}R_2 - K_{23}R_2 + K_{32}R_3. \tag{A4}$$

Therefore: $$R_2 = \frac{1}{(K_{21}+K_{23})}\left(J_{12}X_1 + K_{32}R_3 - \frac{dR_2}{dt}\right). \tag{A5}$$

Substituting (A5) in (A3) gives:

$$\frac{dR_{2+3}}{dt} = J_{12}X_1 - \frac{K_{21}}{K_{21}+K_{23}}\left(J_{12}X_1 + K_{32}R_3 - \frac{dR_2}{dt}\right). \tag{A6}$$

The major assumption of the model is that the exchangeable cytosolic pool (Ca_2) is much smaller than the exchangeable organelle pool (Ca_3). Thus, over a period of minutes dR_2/dt, the rate of accumulation of label into the cytosolic pool, will be a negligible fraction of the unidirectional influx of radiolabelled Ca^{2+} into the whole cell, $J_{12}X_1$. It may therefore be eliminated from the right-hand side of eqn. (A6).

Therefore: $$\frac{dR_{2+3}}{dt} = J_{12}X_1\left(1 - \frac{K_{21}}{K_{21}+K_{23}}\right) - \frac{K_{32}K_{21}R_3}{K_{21}+K_{23}}. \tag{A7}$$

Now, $R_3 \sim R_{2+3} = R_T$, which is the total radioactivity in the cell, so that one can write:

$$\frac{dR_T}{dt} = J_{12}X_1\left(1 - \frac{K_{21}}{K_{21}+K_{23}}\right) - \frac{K_{32}K_{21}R_T}{K_{21}+K_{23}}. \tag{A8}$$

(A8) can be solved for R_T *vs.* time using the boundary condition that $R_T = 0$ at $t = 0$:

$$R_T = \frac{J_{12}X_1K_{23}}{K_{21}K_{32}}\left(1 - \exp\frac{[-K_{32}K_{21}t]}{K_{21}+K_{23}}\right). \tag{A9}$$

R_T is the measured uptake of $^{45}Ca^{2+}$ at time t.

This may be converted into Ca^{2+} uptake during time t by writing R_T/X_1 as the Ca^{2+} uptake, Ca_T. (This assumes the specific activity of entering Ca^{2+} equals that of extracellular Ca^{2+}.)

$$Ca_T = \frac{J_{12}K_{23}}{K_{32}K_{21}}\left(1 - \exp\frac{[-K_{32}K_{21}t]}{K_{21}+K_{23}}\right) \tag{A10}$$

$$= A_T\left(1 - \exp\frac{[-K_{32}K_{21}t]}{K_{21}+K_{23}}\right), \tag{A11}$$

where A_T is the steady-state concentration of Ca^{2+}.

The assumption is often made (Borle, 1975; Scheid & Fay, 1984) that $K_{21} \ll K_{23}$. It is not at all clear that this is so; however, if it is, then (A10) reduces to:

$$Ca_T = J_{12}K' (1 - \exp[-K't]), \quad (A12)$$

where $K' = K_{32}K_{21}/K_{23}$ is an apparent efflux rate constant.

In general, though, eqns. (A10) and (A11) define the uptake and $K' = K_{32}K_{21}/(K_{23}+K_{21})$ is the apparent efflux rate constant which is calculated from the fit of the exponential equation to the data (K_1 in Table 1) and (A10) and (A11) are general equivalent expressions for the uptake *vs.* time.

In Table 1, J_{12}, the unidirectional influx, was calculated by assuming it equalled $A_1 \times K_1$. This is equivalent to the condition that $A_T \times K' = J_{12}$ and is true if $K_{21} \ll K_{23}$, as is seen by comparing eqns. (A11) and (A12). However, if this large inequality does not exist then, using (A10) and (A11), it is apparent that $J_{12} \neq K' \times A_T$ because

$$\frac{K_{32}K_{21}}{K_{23}} \neq K'.$$

Rather,

$$J_{12} = A_T K' \left(\frac{K_{21}+K_{23}}{K_{23}}\right).$$

K_{21} and K_{23} are not independently known so that J_{12} is not explicitly calculable in this case. In so far as $K_{21}+K_{23}/K_{23}$ differs from unity the calculated values of J_{12}, in Table 1, will differ from the true unidirectional influxes.

The authors are very grateful for the excellent technical assistance of Cynthia Hurtenbach, Susan Hipp and Miriam Stucker and secretarial work of Carrie Poole and Susan Krey. Supported by grants from the N.I.H. to P.L. and to I.S.K.

REFERENCES

AMES, A. III & NESBETT, F. B. (1983). Pathophysiology of ischemic cell death. III. Role of extracellular factors. *Stroke* **14**, 233–240.

AMTORP, O. (1979). Distribution of inulin, sucrose and mannitol in rat brain cortex slices following *in vivo* or *in vitro* equilibration. *Journal of Physiology* **294**, 81–90.

BAIMBRIDGE, K. G. & MILLER, J. J. (1981). Calcium uptake and retention during long-term potentiation of neuronal activity in the rat hippocampal slice preparation. *Brain Research* **221**, 299–305.

BARRITT, G. J., PARKER, J. C. & WADSWORTH, J. C. (1981). A kinetic analysis of the effects of adrenaline on calcium distribution in isolated rat liver parenchymal cells. *Journal of Physiology* **312**, 29–55.

BELLOMO, G., NICOTERA, P. & ORRENIUS, S. (1984). Alterations in intracellular calcium compartmentation following inhibition of calcium efflux from isolated hepatocytes. *European Journal of Biochemistry* **144**, 19–23.

BLACKWELL, G. J., FLOWER, R. J., NIJKAMP, F. P. & VANE, J. R. (1978). Phospholipase A_2 activity of guinea-pig isolated perfused lungs: stimulation and inhibition by anti-inflammatory steroids. *British Journal of Pharmacology* **62**, 79–89.

BORLE, A. B. (1969). Kinetic analysis of calcium movements in Hela cell cultures. I. Calcium influx. *Journal of General Physiology* **55**, 43–56.

BORLE, A. B. (1970). Kinetic analysis of calcium movement in cell cultures. III. Effects of calcium and parathyroid hormones in kidney cells. *Journal of General Physiology* **55**, 163–178.

BORLE, A. B.(1975). Methods for assessing hormone effects on calcium fluxes *in vitro*. *Methods in Enzymology* **39**, 513–573.

COOKE, W. J. & ROBINSON, J. D. (1971). Factors influencing calcium movements in rat brain slices. *American Journal of Physiology* **221**, 218–225.

CROMPTON, M., MOSER, R., LUDI, H. & CARAFOLI, E. (1978). The interrelations between the transport of sodium and calcium in mitochondria of various mammalian tissues. *European Journal of Biochemistry* **82**, 25–31.

DIPOLO, R. (1979). Calcium influx in internally dialysed squid giant axons. *Journal of General Physiology* **73**, 91–113.

GILL, D. L., GROLLMAN, E. F. & KOHN, L. (1981). Calcium transport mechanisms in membrane vesicles from guinea pig brain synaptosomes. *Journal of Biological Chemistry* **256**, 184–192.

HAPPEL, R. D., BANIK, N. L., BALENTINE, D. & HOGAN, E. L. (1984). Tissue calcium levels in $CaCl_2$-induced myelopathy. *Neuroscience Letters* **49**, 279–283.

HARRIS, R. J., SYMON, L., BRANSTON, N. M. & BAYHAN, M. (1981). Changes in extracellular calcium activity in cerebral ischemia. *Journal of Cerebral Blood Flow and Metabolism* **1**, 203–209.

HASS, W. K. (1981). Beyond cerebral blood flow; metabolism and the ischemic threshold: an examination of the role of calcium in cerebral infarction. *Cerebral Vascular Disease* **3**, 3–17.

HELLMAN, B. (1978). Calcium and pancreatic b-cell function. 3. Validity of the La-wash technique for discriminating between superficial and intracellular ^{45}Ca. *Biochimica et biophysica acta* **540**, 534–542.

KASS, I. S. & LIPTON, P. (1982). Mechanisms involved in irreversible anoxic damage to the *in vitro* hippocampal slice. *Journal of Physiology* **332**, 459–472.

KASS, I. S. & LIPTON, P. (1983). Differential sensitivity of pyramidal and granule cell neurons to anoxic damage in hippocampi from young rats. *Neuroscience Abstracts* **9**, 473.

KEYKHAH, M. M., WELSH, F. A., MILLER, A. S., HARP, J. R. & DEFEO, S. P. (1978). Calcium energy metabolite levels and survival following exposure to low inspired oxygen concentration. *Critical Care Medicine* **6**, 330–334.

KOOMEN, J. M., SCHEVERS, J. A. M. & NOORDHOCK, J. (1983). Myocardial recovery from global ischemia and reperfusion: effects of pre and/or post-ischemic perfusion with low-Ca. *Journal of Molecular and Cellular Cardiology* **15**, 383–392.

LIBBY, P. & GOLDBERG, A. L. (1978). Leupeptin, a protease inhibitor decreases protein degradation in normal and diseased muscles. *Science* **199**, 534–536.

LIPTON, P. & HEIMBACH, C. J. (1977). The effect of extracellular potassium on protein synthesis in guinea-pig hippocampal slices. *Journal of Neurochemistry* **28**, 1347–1354.

LIPTON, P. & HEIMBACH, C. J. (1978). The mechanism of extracellular potassium stimulation of protein synthesis in guinea-pig hippocampal slices. *Journal of Neurochemistry* **31**, 1299–1308.

LIPTON, P. & WHITTINGHAM, T. S. (1979). The effect of hypoxia on evoked responses in the *in vitro* guinea-pig hippocampus. *Journal of Neurophysiology* **325**, 51–65.

LUST, W. D., FEUSSNER, E. K., BARBEHENN, E. K. & PASSONNEAU, J. V. (1982). The enzymatic measurement of adenine nucleotides and P-creatine in picomole amounts. *Analytical Biochemistry* **1100**, 258–266.

MELDRUM, B. S. (1981). Metabolic effects of prolonged epileptic seizures and the causation of epileptic brain damage. In *Metabolic Disorders of the Nervous System*, ed. ROSE, F. C., pp. 175–187. London: Pitman.

MORIARTY, C. M. (1980). Kinetic analysis of calcium distribution in rat anterior pituitary slices. *American Journal of Physiology* **238**, E167–173.

MYERS, R. E. (1981). Brain damage due to asphyxia: mechanism of causation. *Journal of Perinatal Medicine* **9**, suppl. 1, 78–86.

PERNEY, T. M., DINERSTEIN, R. J. & MILLER, R. J. (1984). Depolarization-induced increases in intracellular free calcium detected in single cultured neuronal cells. *Neuroscience Letters* **51**, 165–170.

PETITO, C. K. & PULSINELLI, W. A. (1984). Delayed neuronal recovery and neuronal death in rat hippocampus following severe cerebral ischemia: possible relationships to abnormalities in neuronal processes. *Journal of Cerebral Blood Flow and Metabolism* **4**, 194–205.

PULSINELLI, W. A., BRIERLY, J. B. & PLUM, F. (1982). Temporal profile of neuronal damage to a model of transient forebrain ischemia. *Annals of Neurology* **11**, 491–498.

REHNCRONA, S., ROSEN, I. & SIESJO, B. K. (1981). Brain lactic acidosis and ischemic cell damage. I. Biochemistry and neurophysiology. *Journal of Cerebral Blood Flow and Metabolism* **1**, 297–311.

ROTHMAN, S. (1984). Synaptic release of excitatory amino-acid neurotransmitters mediates anoxic neuronal death. *Journal of Neuroscience* **4**, 1884–1891.

SCHEID, C. R. & FAY, F. S. (1984). Transmembrane ^{45}Ca fluxes in isolated smooth muscle cells: basal Ca fluxes. *American Journal of Physiology* **246**, C422–430.

SIEMKOWICZ, E. & HANSON, A. J. (1981). Brain extracellular ion composition and EEG activity following 10 minutes of ischemia in normo- and hyperglycemic rats. *Stroke* **12**, 236–240.

SIESJO, B. K. (1981). Cell damage in the brain: a speculative synthesis. *Journal of Cerebral Blood Flow and Metabolism* **1**, 155–185.

SIMON, R. P., SWAN, J. H., GRIFFITHS, T. & MELDRUM, B. S. (1984). Blockade of *N*-methyl-D-aspartate receptors may protect against ischemic damage in brain. *Science* **226**, 850–852.

SMITH, M. L., KAGSTROM, E., ROSEN, I. & SIESJO, B. K. (1983). Effect of the calcium antagonist nimodipine on the delayed hypoperfusion following incomplete ischemia in the rat. *Journal of Cerebral Blood Flow and Metabolism* **3**, 543–546.

SNELLING, R. & NICHOLLS, D. (1985). Calcium efflux and cycling across the synaptosomal plasma membrane. *The Biochemical Journal* **226**, 225–231.

STAHL, W. L. & SWANSON, P. D. (1972). Calcium movements in brain slices in low sodium or calcium media. *Journal of Neurochemistry* **19**, 2395–2407.

STAUBLI, U., BAUDRY, M. & LYNCH, G. (1984). Leupeptin, a thiol protease inhibitor, causes a selective impairment of spatial maze performance in rats. *Behavior and Neural Biology* **40**, 58–69.

SZERB, J. C., ROSS, E. T. & GUREVICH, L. (1981). Compartments of labeled and endogenous γ-aminobutyric acid giving rise to release evoked by potassium or veratridine in rat cortical slices. *Journal of Neurochemistry* **37**, 1186–1192.

VAN BREEMEN, C., FARINAS, B. R., CASTEELS, R., GREBA, P., WUTTACK, F. & DETH, R. (1973). Factors controlling cytoplasmic Ca concentration. *Philosophical Transactions of the Royal Society B* **265**, 57–71.

VON LUBITZ, D. K. & DIEMER, N. H. (1983). Cerebral ischemia in the rat: ultrastructural and morphometric analysis of synapses in stratum radiatum of the hippocampal CA region. *Acta neuropathologica* **61**, 52–60.